Journal of Mechanical Engineering and Sciences
ISSN (Print): 2289-4659; e-ISSN: 2231-8380
Volume 13, Issue 3, pp. 5513-5527, September 2019

DOI: https://doi.org/10.15282/jmes.13.3.2019.19.0445

Predictive tool for frictional performance of piston ring-pack/liner conjunction

J. W. Tee[1], S. H. Hamdan[2*], and W. W. F. Chong[1,3]

[1]School of Mechanical Engineering, Faculty of Engineering,
Universiti Teknologi Malaysia, 81310 Johor Bahru, Johor, Malaysia,
[2]Section of Bioengineering Technology,
University Kuala Lumpur Malaysia Institute of Chemical & Bioengineering Technology,
Taboh Naning, 78000 Alor Gajah, Melaka, Malaysia
[3]UTM Centre for Low Carbon Transport in Cooperation with Imperial College London,
School of Mechanical Engineering, Faculty of Engineering, Universiti Teknologi Malaysia,
81310 Johor Bahru, Johor, Malaysia
*Email: sitihartini@unikl.edu.my

ABSTRACT

A substantial portion of engine frictional losses come from piston-ring assembly. However, accurately measuring in-cylinder frictional losses under actual engine operation remains a challenge to the automotive industry, especially during design stages of engines. Hence, the study proposes a simplistic mathematical tool to simulate the effect of different piston ring profiles towards engine in-cylinder friction. The models are derived from Reynolds equation to determine contact pressure generated by the lubricant film formed between the ring and the liner. Friction generated by the ring pack is then computed using Greenwood and Williamson's rough surface contact model. It is found that friction from the top compression ring is the largest, followed by the second compression ring and the oil control ring (single rail), with total friction of 301.3 N. On top of this, emphasis should also be placed on the top compression ring because of its direct exposure towards the combustion chamber in the engine. The predicted film thickness and friction force also showed correlation to other models reported in literature. Hence, the proposed predictive tool prepares for a simple yet robust platform in predicting frictional losses of piston ring-pack/liner conjunction, allowing for improved fundamental understanding of internal combustion engine in-cylinder lubrication.

Keywords: Piston ring-pack; lubrication; engine in-cylinder friction; Reynolds' equation; rough surface contact model.

INTRODUCTION

Environmental concerns on greenhouse gas (GHG) emission and energy cost have led to the development of more efficient components and systems for vehicle manufacturers. It is estimated that within the next 25 years, the global energy demand is expected to increase by almost 33%, from 588 EJ (year 2014) to 742 EJ (year 2040) [1]. According to Holmberg et al. [2], approximately 20% of the global annual energy demand are utilized in overcoming friction generated by passenger cars. It is estimated that only 17.5% of the total fuel energy

is left behind to move the vehicle [3]. Frictional losses in an internal combustion engine contribute between 4% and 15% of the fuel consumption in passenger cars [4], with the piston ring–cylinder system contributing up to 40–45% of these losses [5].

Typical piston ring/liner operation in an internal combustion engine undergoes a wide range of lubrication regimes during operation [6,7]. For a complete engine cycle of 4-strokes, hydrodynamic viscous shearing appears to dominate along the intake and the exhaust stroke. While at the reversal position of power and compression stroke, the lubrication regime would typically shift towards mixed and boundary lubrication regime. From this observation, it can be surmised that friction generated by the piston ring/liner contact would typically be as a result of the combination of Poiseuille shear and also surface asperity interaction along two opposing sliding surfaces [8].

With the piston ring-pack/liner system dominating energy losses in internal combustion engines due to friction, it is imperative that an improved fundamental understanding with relation to the ring/liner lubrication mechanism be obtained in order to reduce fuel consumption of these engines. In an engine, the piston ring pack typically comprises of different types of rings, where each ring has a specific operating condition with unique contact geometry. During cyclic operation of the piston motion, within the ring-pack itself, the lubricant at the entrainment inlet is influenced by the lubricant amount at the entrainment outlet of the previous ring. Therefore, fully flooded condition might occur only along the top compression ring in which the subsequent rings might operate under lubrication starved condition.

Numerous methods have been adopted experimentally to measure friction generated by the piston ring/liner conjunction [9-11]. Most of the methods require extensive modifications of the engine. Recently, with minimal engine modification, Fang et al. [12] proposed an improved technique, based on wireless telemetry technology, to measure piston ring/liner friction under motored condition. They compared their results with numerical solutions for the piston ring pack, which generated peak friction force between 100 N and 300 N at varying engine speeds. However, the details of the piston ring profiles are not provided in their paper, making it difficult to replicate their simulation results.

Measuring friction of piston ring/liner has been shown to be possible. However, such approach still requires a significant amount of resources in effectively solving the challenges faced during setup of the test engine. Therefore, it is essential that a predictive approach be developed to complement and better aid the design of engine in-cylinder lubrication system. Numerous research work has been done to simulate the piston ring/liner lubrication system. A common method used to calculate the lubricant film thickness is by solving for Reynolds equation. This is used to correlate contact geometry, relative sliding velocity of opposing surfaces, lubricant properties (viscosity and density) and normal load within a lubrication system. The different profiles of the piston rings are also expected to affect lubricant entrainment into the ring/liner contact. This will impact the formation of lubricant film or film thickness, which acts to minimize the ring-pack/liner friction. An example includes the work by Miltsios et al. [13], where they employed the Finite Element Method (FEM) in order to: 1) solve for the governing equations for piston ring/liner lubrication system and 2) determine the friction force generated by each ring. Recently, Zhao et al. [14] also implemented the FEM in analysing the piston ring/liner tribological conjunction.

Alternatively, Jeng [15] analysed the lubrication performance of a piston ring pack/liner contact based on Reynolds equation. Jeng [15] also considered the effect of

varying engine speed and different piston ring face profile for the first and the second compression ring. Similar approach based on Reynolds solution has also been adopted by Rahmani et al. [16] for new and worn top compression piston rings. Recently, Chong et al. [17] applied a modified Elrod's cavitation algorithm in modifying Reynolds equation to consider the effect of cavitation towards piston ring/liner frictional characteristics. Both the above studies have shown that worn rings generated an increased oil film thickness, thus, leading to lower friction along engine cylinder liner. However, care must be taken into consideration for such situation because excessive wear of the piston ring could have adverse effects towards frictional properties of the piston ring/liner contact, incurring undesirable energy losses.

Reynolds solution could only provide information on the contact pressure and the thickness of the lubricant film. In order to determine the friction from Reynolds solution, rough surface contact models are applied. The most commonly used rough surface contact model originated from Greenwood and Williamson's model [18]. The model has been extended for engine tribology application, such as the ones reported by Teodorescu et al. [19]. Their model considered viscous and boundary friction components along rough surface contacts. This model has also been applied by Chong et al. [20] in determining the friction force along a piston ring/liner contact. More detailed rough surface contact model based on the concept of fractal geometry, such as the ones proposed by Chong et al. [19] and Miao and Huang [21], could also be applied for a ring/liner contact.

Piston ring/liner contact has been shown to have a significant impact towards the frictional lost per unit contact are due to friction and wear performance. To reduce friction and wear generated along the ring/liner tribological conjunction, one of the most proposed approach is to introduce textures on the ring or the liner surface. Studies have found that having micro-dimples along the piston ring surface could reduce friction up to 25% [22, 23]. It was also observed that when surface textures are introduced to the liner, up to 4.5% of friction reduction could be achieved [24]. On the other hand, Vlădescu et al. [25] investigated the effect of cavitation towards a laser textured piston ring/liner contact. They found that the surface textures created prevent lubricant starvation at piston motion reversal points and also act to reduce burning of lubricant at top dead centre. In simulating the effect of surface textures towards piston ring/liner contact, Gu et al. [26] and Morris et al. [27] solved for a one-dimensional average Reynolds equation. The averaged Reynolds solution for such analysis are often derived numerically, which could be computationally expensive and time consuming. Aside from having surface textures, improvement on lubricants used along the piston ring/liner conjunction could also be done by introducing nanoparticles as boundary lubricants [28-30].

It is important to comprehend the friction mechanism across the piston ring-pack/liner conjunction in order to more effectively reduce cylinder frictional losses. Accurately measured frictional losses of piston ring pack under actual engine operating conditions are scarce. This presents a challenge to the automotive industry during the design stage of engines. A useful solution is to resort to predictive tools. However, most of the reported predictive tools available are numerical based and involves significant amount of computational cost. On top of this, the investigation reported is most often only about the top compression ring. Therefore, this study intends to derive a simplistic predictive tool by extending the work by Ng et al. [31] to determine the frictional performance for a complete piston ring-pack/liner conjunction. Through this approach, it is expected that a simplistic

mathematical platform be proposed to ease the fundamental understanding of piston ring-pack/liner tribological behaviour along a whole engine cycle operation in an internal combustion engine.

MATHEMATICAL APPROACH

The present study derives an analytical solution in predicting the tribological properties of a piston ring-pack/liner conjunction. The mathematical modelling approach are divided into two stages. The first stage requires the derivation of a 1-D Reynolds solution in predicting the lubricant film thickness generated along the ring/liner contact. Then, using the predicted film thickness, the second stage implements the Greenwood and Williamson's rough surface contact model in determining the frictional behaviour along the ring/liner sliding conjunction for the whole engine cycle operation.

1-D Reynolds Solution for Complete Piston Ring-Pack

Reynolds' equation is commonly utilized for piston ring/liner analysis to determine the contact pressure and the lubricant film thickness. In this analysis, it is assumed that the contact pressure generated by the lubricant will not alter the lubricant rheological properties (e.g. viscosity and density). As an initial approximation, long bearing assumption is taken in solving for the Reynolds equation because the ratio of ring circumferential length towards ring width is more than 100 [17]. Therefore, the iso-viscous pressure distribution along the piston ring and engine cylinder liner conjunction can be predicted using the 1-D Reynolds' equation as given below:

$$\frac{\partial}{\partial x}\left(\frac{h^3}{\eta}\frac{\partial P}{\partial x}\right) = 12\left\{\frac{\partial}{\partial x}\frac{(U_1+U_2)}{2}.h + (W_{s1}-W_{s2})\right\} \quad (1)$$

where h refers to the thickness of the lubricant film, P refers to the contact pressure, η refer to the lubricant dynamic viscosity, $(U_1+U_2)/2$ refers to the lubricant entrainment velocity, $(W_{s1}-W_{s2})$ refers to the squeezing action and x is the ring width.

In this study, the profile for the piston top compression ring and the second compression ring are assumed to be parabola and tapered in shape, respectively. On the other hand, the oil control rings consist of a pair of symmetrical parabolic rings [15]. These ring face profiles can sufficiently be represented using a barrel-shaped ring assumption [15]. Hence, a generalised equation, describing the different geometry of the piston rings, h_s is given as follow:

$$h_s(x) = \frac{c}{\left(\frac{b}{2}+o\right)}(x-o)^2 \quad (2)$$

where c refers to the crown height, o refers to the crown offset and b refers to the width of the piston ring. The schematic diagram representative of the simulated ring profile is given in Figure 1. The lubrication film thickness, h can then be expressed as below:

$$h(x) = h_o + h_s(x) \quad (3)$$

Where h_o is the minimum lubricant film thickness.

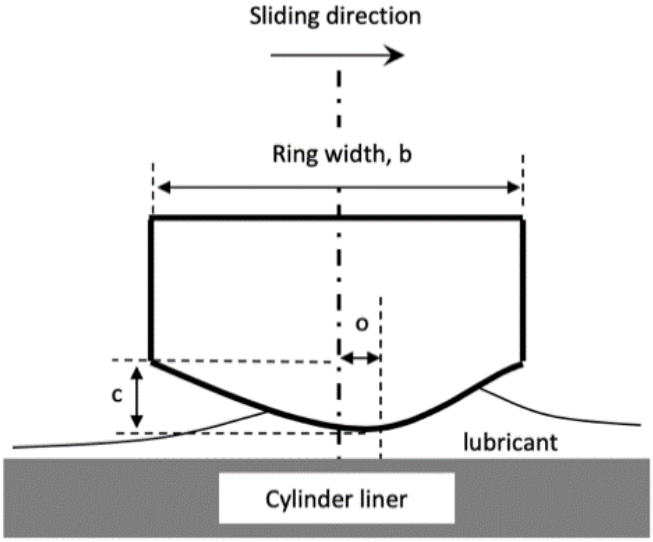

Figure 1. Diagram of the simulated piston ring/liner tribological conjunction.

To solve for Equation (1), it is assumed that $\eta=\eta_0$, $U = U_1 + U_2$ and $W_S=W_{S1}-W_{S2}$. Thus, Equation (1) is modified and integrated as follow:

$$h^3 \frac{\partial P}{\partial x} = 6U\eta_o h + 12W_s\eta_o x + C_1 \tag{4}$$

To determine C_1 for Equation (4), Reynolds boundary condition is applied, where the derivative of contact pressure is taken to be zero at the point of rupture, x_l, where the contact pressure is at its minimum point. At this location, the film thickness is annotated as h_l, which refers to the film thickness at rupture point. This first boundary condition is written as:

$$\frac{\partial P}{\partial x} = 0 \tag{5}$$

where $x = x_l$ and $h = h_l$. By applying this boundary condition, Equation (4) can now be written as below:

$$\frac{\partial P}{\partial x} = \frac{6U\eta_0(h - h_l)}{h^3} + \frac{12W_s\eta_0(x - x_l)}{h^3} \tag{6}$$

Before integrating Equation (6) to obtain the solution for the Reynolds equation, non-dimensional terms, as given below, are applied together with the defined film thickness given in Equation (3).

$$tan\bar{x} = \sqrt{\frac{c}{h_o}}\left(\frac{x-o}{\frac{b}{2}+o}\right) \qquad tan\bar{x}_l = \sqrt{\frac{c}{h_o}}\left(\frac{x_l-o}{\frac{b}{2}+o}\right)$$

$$\bar{h}_o = \frac{h_o}{c} \qquad \bar{o} = \frac{o}{c} \qquad \bar{b} = \frac{b}{c}$$

$$\bar{P} = \frac{h_o^{\frac{3}{2}}\mathrm{P}}{6U\eta_o c^{\frac{1}{2}}} \qquad \bar{W}_s = \frac{W_s}{U}$$

This gives the non-dimensional pressure, $\bar{P}$ equation as follow:

$$\bar{P} = \left(\frac{\bar{b}}{2} + \bar{o}\right)\left[\frac{1}{8}\bar{x} - \frac{1}{32}sin4\bar{x} - tan^2\bar{x}_l\left(\frac{3}{8}\bar{x} + \frac{1}{4}sin2\bar{x} + \frac{1}{32}sin4\bar{x}\right)\right. \\ - \frac{2\bar{W}\left(\frac{\bar{b}}{2} + \bar{o}\right)}{\sqrt{\bar{h}_0}}\left\{\frac{3}{32} + \frac{1}{8}cos2\bar{x} + \frac{1}{32}cos4\bar{x}\right. \\ + tan\bar{x}_l\left(\frac{3}{8}\bar{x} + \frac{1}{4}sin2\bar{x}\right. \\ \left.\left. + \frac{1}{32}sin4\bar{x}\right)\right\} - \frac{1}{8}\tan^{-1}\left(-\sqrt{\frac{1}{\bar{h}_0}}\right) \\ + \frac{1}{32}sin4\left(\tan^{-1}\left(-\sqrt{\frac{1}{\bar{h}_0}}\right)\right) \\ + tan^2\bar{x}_l\left(\frac{3}{8}\tan^{-1}\left(-\sqrt{\frac{1}{\bar{h}_0}}\right)\right. \\ + \frac{1}{4}sin2\left(\tan^{-1}\left(-\sqrt{\frac{1}{\bar{h}_0}}\right)\right) \\ \left. + \frac{1}{32}sin4\left(\tan^{-1}\left(-\sqrt{\frac{1}{\bar{h}_0}}\right)\right)\right)\Bigg] \tag{7}$$

In order to obtain the generated contact pressure along the ring/liner conjunction, it is essential to ascertain the rupture point, x_l. To determine the rupture point, $\bar{x}_l$ in Equation (7), the non-dimensional pressure, $\bar{P}$ at $x = x_l$ is set to zero. Once the contact pressure is calculated for a given minimum film thickness, the load carried by the piston ring can be obtained using:

$$W = \int_{inlet}^{outlet} P \; dx \cdot L \tag{8}$$

Friction Force

To calculate the friction force, lubricant film thickness for the piston ring/liner is required. The lubricant film thickness profile obtained above is used as the input to predict the friction force along piston ring/liner contact. For the present study, the Greenwood and Williamson model is implemented using the analytical method proposed by Teodorescu et al. [19]. Their simplistic model considers the friction force to consist of two components: 1) lubricant viscous shearing component (f_v) and 2) boundary shearing component (f_b) arising from direct surface asperity interaction. Thus, the friction force for an element area (dA) of the piston ring/liner contact is given as:

$$df_f = df_b + df_v \tag{9}$$

For an area of grid element, the lubricant viscous friction force when the fluid is Newtonian in behaviour is computed as:

$$df_v = \tau(dA - dA_a) \tag{10}$$

where $\tau = \eta V/h(x)$ with V being the sliding velocity and dA_a being the asperity contact area. The term τ refers to the shear stress. Hence, the viscous shear component, τ_v is computed as:

$$\tau_v = \frac{\eta V}{h(x)} . \frac{(dA - dA_a)}{dA} \tag{11}$$

When the lubricant film is too thin, boundary friction becomes significant, which could possibly lead to the shearing along interacting asperity tips. In this case, the boundary shear can be predicted using Eying model [19]:

$$df_b = dA_a \left(\tau_o + m\frac{dW_a}{dA_a}\right) \tag{12}$$

where τ_o refers to the lubricant Eyring stress, m refers to the lubricant boundary shear strength coefficient while dW_a refers to the load supported by the asperities for an element's area. The asperity contact area, dA_a and load applied on the asperities, dW_a can be predicted using the Greenwood and Williamson model as follow:

$$dA_a = \pi^2(\zeta\beta\sigma)^2 dA f_2(\lambda)$$
$$dW_a = \frac{8\sqrt{2}}{15}\pi(\zeta\beta\sigma)^2\sqrt{\frac{\sigma}{\beta}}E^* dA f_{5/2}(\lambda) \tag{13}$$

With these two statistical functions, $f_2(\lambda)$ and $f_{5/2}(\lambda)$, being defined according to the two functions proposed by Teodorescu et al. [16], which are:

$$f_2(\lambda) = -0.116\lambda^3 + 0.4682\lambda^2 - 0.7949\lambda + 0.4999$$
$$f_{5/2}(\lambda) = -0.1922\lambda^3 + 0.721\lambda^2 - 1.0649\lambda + 0.6163 \tag{14}$$

where the separation parameter, $\lambda = h(x)/\sigma$. The term σ is the combined asperity of piston ring/liner contact surfaces and the composite elastic modulus of the two materials, E^* are determined as follow:

$$\frac{1}{E^*} = \frac{1}{2}\left[\frac{1 - {v_1}^2}{E_1} + \frac{1 - {v_2}^2}{E_2}\right] \tag{15}$$

with v_1 and v_2 are the Poissons' ratios, E_1 and E_2 are the modulus of elasticity for the material of the piston ring and cylinder liner. Using the Greenwood and Williamson rough surface contact model, the total friction force along the piston ring/liner contact can then be computed as follow:

$$f_{total} = \int_{inlet}^{outlet} (df_b + df_v)\ dx \cdot L \tag{16}$$

RESULTS AND DISCUSSIONS

The present study simulates the tribological properties of a complete piston ring-pack sliding along the engine cylinder liner during an engine cycle operation. Most of the simulated parameters are taken from the work of Jeng [10]. Figure 2 illustrates the essential simulated conditions for the ring/liner conjunction, where the sliding velocity is determined as given by Chong et al. [17]. The normal load applied on the ring is due to 1) the combustion pressure, as given in Figure 2 (b), flowing to the back of the ring and 2) the ring elastic pressure due to ring tension. The ring tension is required to effectively seal the combustion chamber to reduce blow-by effect. At equilibrium condition, the contact pressure generated by the ring/liner is taken to be the sum between the piston ring tension and the combustion pressure acting at the back of the ring.

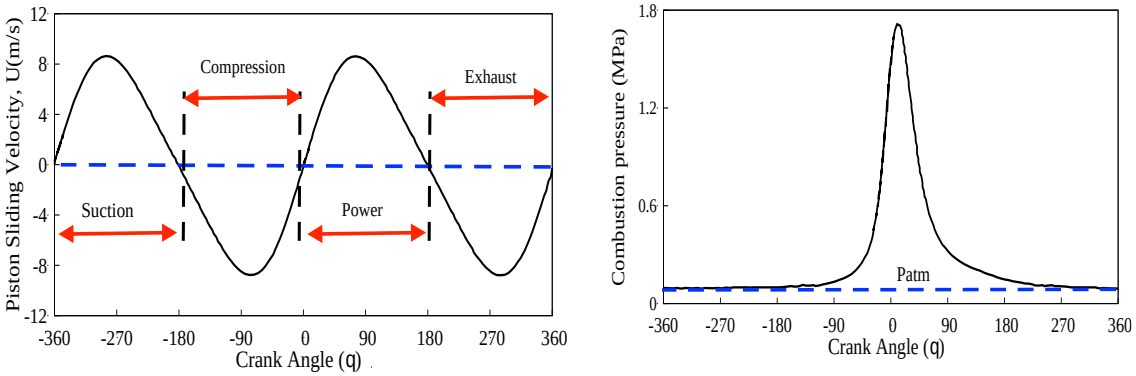

(a) (b)

Figure 2. Simulated conditions for piston ring-pack/liner at engine speed of 2000 rpm (a) Piston sliding velocity, (b) Combustion pressure

Top Compression Ring

The derived Reynolds solution is used to simulate the contact pressure and lubricant film formation (e.g. film thickness) for the top compression ring. Figure 3 displays the predicted contact pressure distribution along the piston ring/liner contact at -40º crank angle during compression stroke. The lubricant film formation is also predicted at this operating condition. It can be observed that at this crank angle, the pressure is hydrodynamic in nature, with film thickness approximately 2 μm. Such lubricant film thickness is much larger than the surface roughness value 0.37 μm. Hence, no boundary interaction is expected.

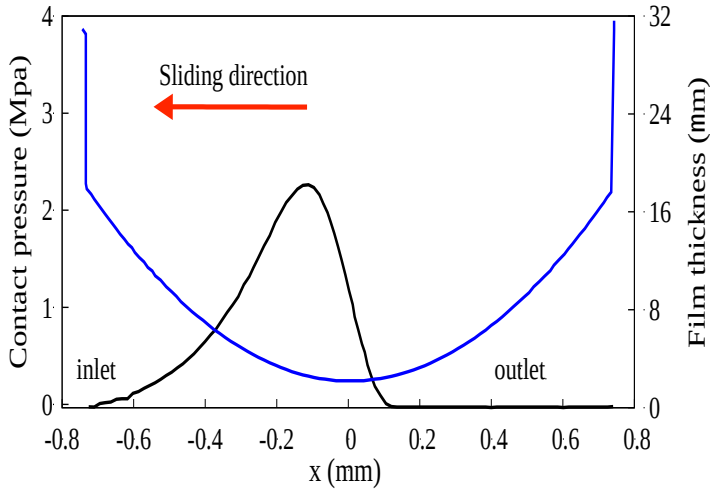

Figure 3. Contact pressure and film thickness generated by top compression ring at -40° crank angle

Based on the simulation above, the lubricant film thickness at each crank angle can then be computed for the top compression ring for the whole engine cycle. The lubricant film thickness at each crank angle is vital in examining the frictional behaviour along the ring/liner contact. Figure 4 (a) illustrates the minimum thickness of the lubricant film for the top compression ring during an engine cycle operation. The largest film thickness of approximately 3.3 µm is predicted is along mid-stroke span. It is noticeable also that the lubricant's minimum film thickness is near zero along all motion reversal regions. This is because when approaching the dead centres, piston motion slows down before changes direction, leading to slow lubricant entrainment into the contact. It is also being shown that the simulation of lubricant minimum film thickness in this study follows the similar pattern given in the literature data by Jeng [10], except along the motion reversal regions. This is because the method reported in the literature limits the film thickness to the composite surface roughness value 0.37 µm. Such assumption also limits the boundary lubrication analysis, where surface asperity interactions become significant.

Before establishing the friction force, shear stress distribution at the piston top compression ring and liner conjunction is first determined. The simulated shear stress consists of two components, namely boundary shear stress and viscous shear stress. By summing up the viscous and boundary friction force at the piston ring and the liner conjunction, the total friction force over complete engine cycle can be computed as shown in Figure 4 (b). It should be noted that along the vicinity of power stroke, highest friction force of around 99.5 N is observed. This is mainly because of the higher load imposed on the ring due to highest combustion pressure during ignition. It can also be observed that the trend of the predicted total friction force for top compression ring correlates well with the trend in literature data [10]. The slightly lower friction force values along the dead centre reversal regions reported in literature [10] are believed to be as a result of the limiting minimum film thickness introduced. This eventually leads to a thicker film estimation at the dead centres as compared to the values predicted by the current study, which applies Greenwood and Williamson's rough surface contact model.

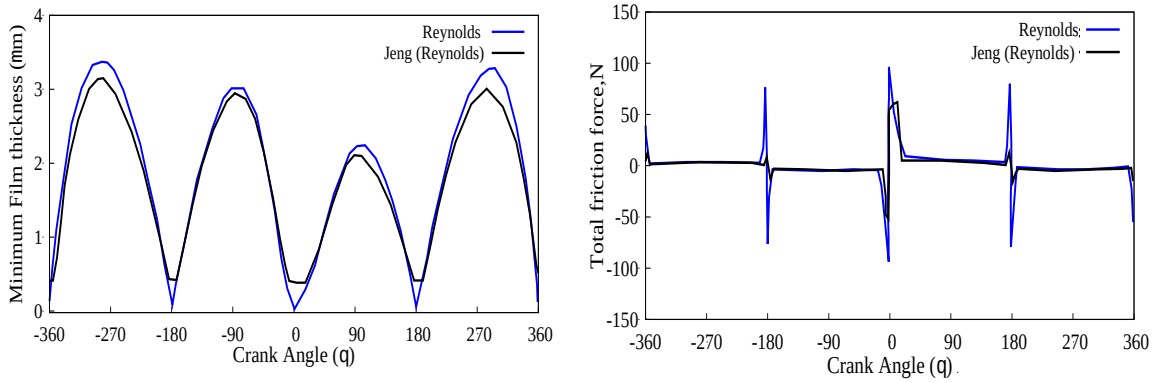

(a) (b)

Figure 4. Comparison of predicted and literature data for (a) minimum film thickness and (b) total friction generated along top compression ring for a complete engine cycle

Second compression ring

In order to simulate the lubricant film thickness profile for the second compression ring, the sliding direction of the ring must be considered because this ring profile is not symmetrical. Figure 5 displays the predicted contact pressure distribution along the piston second compression ring/liner contact for operating conditions at crank angles -40º and 40º. The contact pressure is shown to spread along a narrower region at crank angle 40º because of the smaller convex region along the inlet of the contact. Unlike the symmetrical top compression ring, the narrower convex region for the second compression ring limits the amount of lubricant entrained into the contact, which could induce lubricant starvation, possibly leading to higher friction due to a lack of lubricant. This could also be even more evident considering that the lubricant supply for the second compression ring depends on the left-over lubricant at the trailing edge of the top compression piston ring.

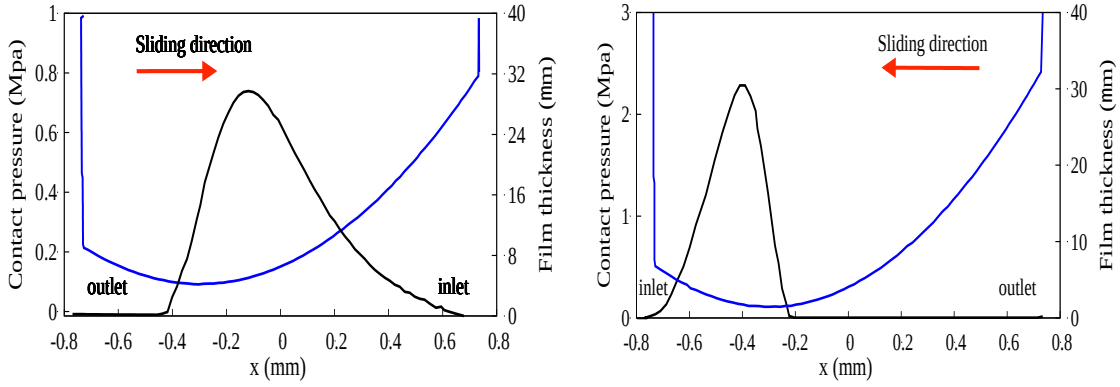

(a) (b)

Figure 5. Contact pressure and film thickness generated by second compression ring at (a) -40°, (b) 40° crank angle

Figure 6 (a) shows the minimum lubricant film thickness of the second compression ring at different crank angles of the whole engine cycle operation. As explained earlier, sliding direction of second compression ring has to be taken into consideration due to its non-symmetrical nature. For the suction and the power stroke, the second compression ring moves downward or towards the negative x direction. For compression and exhaust stroke, the second compression ring moves upward or towards the positive x direction as indicated in Figure 6 (a). The film thickness in the negative x direction is observed to generally be smaller than the one in the positive direction. This is because thicker film is formed when lubricant is entrained into the contact via a larger convex area as compared to a narrower convex area. This leads to the predicted film thickness of up to 7 µm for the second compression ring.

By summing up the viscous and boundary friction force along the second compression ring/liner conjunction, the total friction force over the whole engine cycle is computed as shown in Figure 6 (b). The highest friction is simulated for this ring is around 88.6 N. These values are slightly lower when compared with the friction generated by the top compression ring (see Figure 4). The higher friction force generated by the top ring is as a result of direct exposire towards the combustion chamber, leading to a higher applied normal load. This coupled with the smaller film thickness are essential for the top ring as it is required to have a more effective sealing effect to avoid significant combustion gas blow-by.

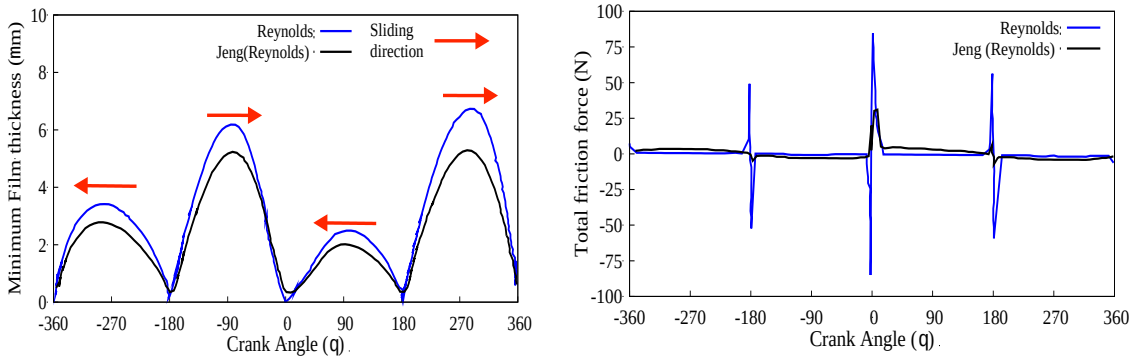

(a) (b)

Figure 6. Comparison of predicted and literature data for (a) minimum film thickness and (b) total friction generated along second compression ring for a complete engine cycle

Oil Control Rings

Another type of piston ring simulated is the oil control ring, which consists of two symmetrical narrow rings, namely upper and lower rail, separated at a fixed distance. The function of oil control rings is to scrape the remaining lubricant along the cylinder liner. These rings are also known as oil scraper rings. Figure 7 shows the predicted contact pressure distribution along the piston oil control ring/liner contact for operating conditions at crank angle -40º. The distance between the upper rail and lower rail used in the simulation is 3.04 mm [10]. Assuming that combustion gas blow-by to be negligible, the load imposed on the oil control rings is expected to be consistent over the whole engine cycle, the entrainment velocity will then be the dominant factor that affects the minimum film thickness and contact pressure. Small entrainment velocity at the vicinity of the dead centres promotes thinner

lubricant film and higher contact pressure, which could lead to higher friction force being generated.

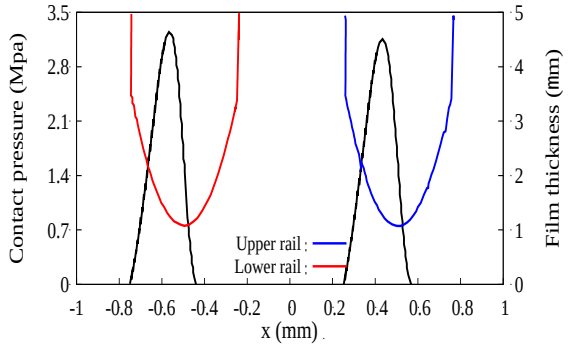

Figure 7. Contact pressure and film thickness generated by oil control ring at -40° crank angle

Figure 8 (a) shows the minimum lubricant film thickness for oil control rings along an engine cycle. It is shown that the simulated lubricant minimum film thickness variation of oil control rings follows the one given in the literature [10], with the largest film thickness simulated to be around 1.3 µm. By summing up the viscous and boundary friction force for the ring/liner contact across the engine cycle, the total friction force over the whole engine cycle can be computed as shown in Figure 8 (b). It is observed that the largest friction force of around 56.6 N (single rail) is generated at the vicinity of all dead centres, where piston motion reversal occurs. This is caused by the low lubricant entrainment velocities when the piston motion changes direction.

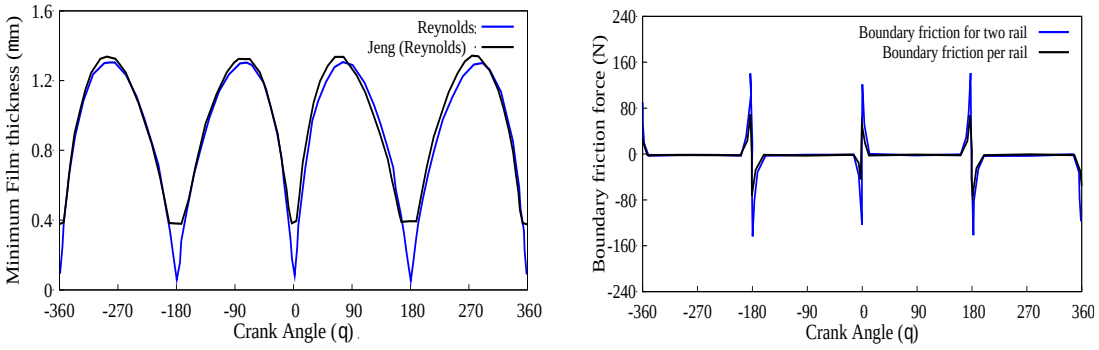

(a) (b)

Figure 8. Comparison of predicted and literature data for (a) minimum film thickness (for a single oil control ring) and (b) total friction generated along the oil control ring for a complete engine cycle

Complete Piston Ring-Pack/Liner

With the frictional properties for each of the rings in a piston ring-pack simulated above, it is now possible to determine the total friction generated by the piston ring-pack along a whole engine cycle. Figure 9 shows the total frictional force of piston rings pack over a complete engine cycle. The largest total friction force is approximately 301.3 N over the whole engine cycle operation, which is found to be around the vicinity of TDC between compression stroke

and power stroke. The predicted value is in the range of total friction measured by Fang et al. [12]. Such observation indicates that the derived predictive tool is capable of reasonably computing the frictional losses of a piston ring pack in an engine.

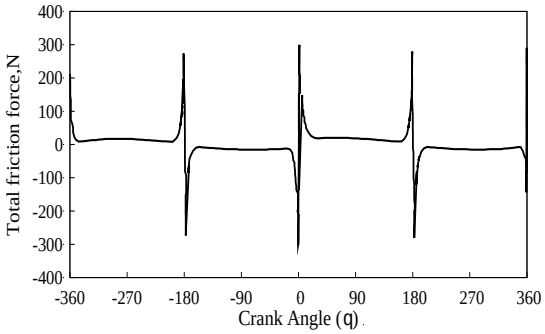

Figure 9. Predicted total friction for a piston ring-pack/liner conjunction

CONCLUSIONS

A simplistic predictive tool is presented, where frictional behaviour of the piston ring pack and the cylinder liner conjunction is simulated. For the ring pack, the film thickness is observed to typically be at its minimum around the dead centre regions during the operation along an engine cycle. This is due to the low piston ring velocity or lubricant entrainment velocity at these locations. The maximum film thickness of the second compression ring is simulated to be the largest (7 µm), followed by the top compression ring (3.3 µm) with the oil control rings having the smallest film thickness (1.3 µm). Greenwood and Williamsons' rough surface contact model is used in this study to ascertain the load carried by surface asperities at the ring and the liner conjunction. The friction force for the top compression ring (99.5 N) is observed to be higher than the second compression ring (88.6 N) and oil control rings (56.6 N per rail) due to its harsh operating condition (direct exposure towards the combustion). From the simulation, it is shown that different ring profiles, such as the offset, crown height and ring width of the rings pack, lead to varied frictional performance of the individual piston rings. The film thickness and the total friction force in this study are compared with literature data, showing reasonable correlation. Hence, it can be concluded that the proposed simplistic Reynolds' solution is capable of simulating the tribological properties of the piston ring-pack/liner conjunction. The predictive tool also prepares for a simplistic mathematical platform to better understand engine in-cylinder frictional losses. The next step forward in further validating this model is to compare the predicted frictional forces with actual measured engine frictional losses under fired conditions.

ACKNOWLEDGEMENT

The authors acknowledge the support provided by the Ministry of Education, Malaysia and Research University Grant (RUG) of Universiti Teknologi Malaysia through the

Transdisciplinary Research Program (TDR) of "Innovative Materials for Resilient Contact Systems (Vot. No.: 06G19 and 05G56)".

REFERENCES

[1] U.S. Energy Information Administration. Retrieved from https://www.eia.gov/outlooks/ieo/pdf/0484(2017).pdf; 10 June, 2019.

[2] Holmberg K, Erdemir A. The impact of tribology on energy use and CO_2 emission globally and in combustion engine and electric cars. Tribology International. 2019.

[3] Chong WWF, Ng JH, Rajoo S, Chong CT. Passenger transportation sector gasoline consumption due to friction in Southeast Asian countries. Energy conversion and management. 2018; 158: 346-358.

[4] Wong VW, Tung SC. Overview of automotive engine friction and reduction trends–Effects of surface, material, and lubricant-additive technologies. Friction. 2016; 1: 1-28.

[5] Tung SC, McMillan ML. Automotive tribology overview of current advances and challenges for the future. Tribology International. 2004; 37(7): 517-536.

[6] Morris N, Mohammadpour M, Rahmani R, Rahnejat H. Optimisation of the piston compression ring for improved energy efficiency of high-performance race engines. Proceedings of the Institution of Mechanical Engineers, Part D: Journal of Automobile Engineering. 2017; 231(13): 1806-1817.

[7] Chong WWF, De la Cruz M. Elastoplastic contact of rough surfaces: a line contact model for boundary regime of lubrication. Meccanica. 2014; 49(5) : 1177-1191.

[8] Shahmohamadi H, Mohammadpour M, Rahmani R, Rahnejat H, Garner CP, Howell-Smith S. On the boundary conditions in multi-phase flow through the piston ring-cylinder liner conjunction. Tribology International. 2015; 90 :164-174.

[9] Mufti RA, Priest M. Experimental evaluation of piston-assembly friction under motored and fired conditions in a gasoline engine. Journal of Tribology. 2005; 127(4) : 826-836.

[10] Gore M, Theaker M, Howell-Smith S, Rahnejat H, King PD. Direct measurement of piston friction of internal-combustion engines using the floating-liner principle. Proceedings of the Institution of Mechanical Engineers, Part D: Journal of Automobile Engineering. 2014; 228(3) : 344-354.

[11] Westerfield Z, Totaro P, Kim D, Tian T. An experimental study of piston skirt roughness and profiles on piston friction using the floating liner engines. SAE Technical Paper. 2016; 1043.

[12] Fang C, Meng X, Xie Y, Wen C, Liu R. An improved technique for measuring piston-assembly friction and comparative analysis with numerical simulations: Under motored condition. Mechanical Systems and Signal Processing. 2019; 115: 657-676.

[13] Miltsios GK, Patterson DJ, Papanastasiou TC. Solution of the lubrication problem and calculation of the friction force on the piston rings. Journal of Tribology. 1989; 111(4): 635-641.

[14] Zhao B, Dai XD, Zhang ZN, Xie YB. A new numerical method for piston dynamics and lubrication analysis. Tribology International. 2016;94 :395-408.

[15] Jeng YR. Theoretical analysis of piston-ring lubrication Part I—fully flooded lubrication. Tribology Transactions. 1992;35(4) :696-706.
[16] Rahmani R, Theodossiades S, Rahnejat H, Fitzsimons B. Transient elastohydrodynamic lubrication of rough new or worn piston compression ring conjunction with an out-of-round cylinder bore. Proceedings of the Institution of Mechanical Engineers, Part J: Journal of Engineering Tribology. 2012; 226(4):284-305.
[17] Chong WWF, Howell-Smith S, Teodorescu M, Vaughan ND. The influence of inter-ring pressures on piston-ring/liner tribological conjunction. Proceedings of the Institution of Mechanical Engineers, Part J: Journal of Engineering Tribology. 2013; 227(2) :154-167.
[18] Greenwood JA, Williamson JP. Contact of nominally flat surfaces. Proc. R. Soc. Lond. A. 1966; 295(1442) :300-319.
[19] Chong WWF, Teodorescu M, Rahnejat, H. Nanoscale elastoplastic adhesion of wet asperities. Proceedings of the Institution of Mechanical Engineers, Part J: Journal of Engineering Tribology. 2013; 227(9) : 996-1010.
[20] Teodorescu M, Taraza D, Henein NA, Bryzik W. Simplified elasto-hydrodynamic friction model of the cam-tappet contact. SAE Technical Paper 2003. 2003;01:0985.
[21] Miao X, Huang X. A complete contact model of a fractal rough surface. Wear. 2014; 309(1-2) :146-151.
[22] Etsion I. Improving tribological performance of mechanical components by laser surface texturing. Tribology letters. 2004; 17(4) : 733-737.
[23] Ryk G, Etsion I. Testing piston rings with partial laser surface texturing for friction reduction. Wear. 2006; 261(7-8) : 792-796.
[24] Rahnejat H, Balakrishnan S, King PD, Howell-Smith S. In-cylinder friction reduction using a surface finish optimization technique. Proceedings of the Institution of Mechanical Engineers, Part D: Journal of Automobile Engineering. 2006;220(9) :1309-1318.1
[25] Vlădescu SC, Ciniero A, Tufail K, Gangopadhyay A, Reddyhoff T. Looking into a laser textured piston ring-liner contact. Tribology International. 2017;115 :140-153.
[26] Gu C, Meng X, Xie Y, Yang Y. Effects of surface texturing on ring/liner friction under starved lubrication. Tribology international. 2016;94 : 591-605.
[27] Morris N, Rahmani R, Rahnejat H, King PD, Howell-Smith S. A numerical model to study the role of surface textures at top dead center reversal in the piston ring to cylinder liner contact. Journal of Tribology. 2016;138(2):021703.
[28] Sahid NSM, Rahman MM, Kadirgama K, Maleque MA. Experimental investigation on properties of hybrid nanofluids (TiO2 and ZnO) in water–ethylene glycol mixture. Journal Of Mechanical Engineering And Sciences. 2017;11: 3087-3094.
[29] Sharma S, Tiwari AK, Tiwari S, Prakash R. Viscosity of hybrid nanofluids: Measurement and comparison. Journal Of Mechanical Engineering And Sciences. 2018; 12 : 3614-3623.
[30] Ng YC, Hamdan SH, Chong WWF. Development of a mathematical tool to predict engine in-cylinder friction. Jurnal Tribologi. 2018; 17:29-39.
[31] Alias AA, Kinoshita H, Nishina Y, Fuji M. Dependence of pH level on tribological effect of graphene oxide as an additive in water lubrication. International Journal of Automotive and Mechanical Engineering. 2016;13: 3150.